

AD-A039 014

MARTIN MARIETTA LABS BALTIMORE MD
GRAIN BOUNDARY SEGREGATION OF A AL-ZN-MG TERNARY ALLOY.(U)
APR 77 J M CHEN, T S SUN, R K VISWANADHAM
MML-TR-77-29C

F/G 11/6

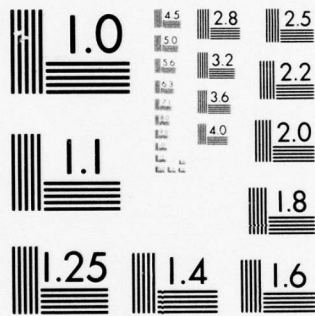
N00014-74-C-0277

NL

UNCLASSIFIED

| OF |
AD
A039014





MICROCOPY RESOLUTION TEST CHART
NATIONAL BUREAU OF STANDARDS-1963-A

ADA039014

MARTIN MARIETTA

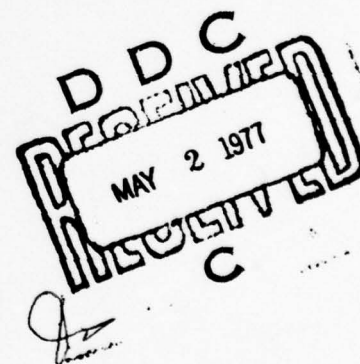
Martin Marietta
Laboratories

9 (12)
MML TR 77-29c

GRAIN BOUNDARY SEGREGATION OF
Al-Zn-Mg TERNARY ALLOY

By
J. M. Chen
T. S. Sun
R. K. Viswanathan
J. A. S. Green

April 1977



Prepared for
Department of the Navy
Office of Naval Research
Arlington, Virginia 22217

Under Contract N00014-74-C-0277,
NR 031-716/11/19/76 (471)

DISTRIBUTION STATEMENT A
Approved for public release;
Distribution Unlimited

MML TR 77-29c

GRAIN BOUNDARY SEGREGATION OF A Al-Zn-Mg TERNARY ALLOY*

by

J. M. Chen, T. S. Sun, R. K. Viswanadham and J.A.S. Green

MARTIN MARIETTA CORPORATION
Martin Marietta Laboratories
1450 South Rolling Road
Baltimore, Maryland 21227

Fourth Technical Report to
OFFICE OF NAVAL RESEARCH
Contract N00014-74-C-0277, NR 031-716/11-19-76 (471)

April 1977

Reproduction in whole or in part is permitted
for any purpose of the United States Government.

Distribution of this document is unlimited.

* This paper has been submitted for publication in
Metallurgical Transactions A.

Unclassified
SECURITY CLASSIFICATION OF THIS PAGE (When Data Entered)

REPORT DOCUMENTATION PAGE		READ INSTRUCTIONS BEFORE COMPLETING FORM
1. REPORT NUMBER MML-TR-77-29c	2. GOVT ACCESSION NO.	3. RECIPIENT'S CATALOG NUMBER
4. TITLE (and Subtitle) GRAIN BOUNDARY SEGREGATION OF A Al-Zn-Mg TERNARY ALLOY,	5. TYPE OF REPORT & PERIOD COVERED Interim Technical Report	
7. AUTHOR(s) J. M. Chen, T. S. Sun, R. K. Viswanadham and J.A.S./Green	8. CONTRACT OR GRANT NUMBER(s) N00014-74-C-0277	
9. PERFORMING ORGANIZATION NAME AND ADDRESS Martin Marietta Corporation Martin Marietta Laboratories 1450 South Rolling Road Baltimore, Maryland 21227	10. PROGRAM ELEMENT, PROJECT, TASK AREA & WORK UNIT NUMBERS NR 031-716/11-19-76	
11. CONTROLLING OFFICE NAME AND ADDRESS Department of the Navy Office of Naval Research (Code 471) Arlington, Virginia 22217	12. REPORT DATE Apr 1977	
14. MONITORING AGENCY NAME & ADDRESS (if different from Controlling Office)	13. NUMBER OF PAGES 27	
	15. SECURITY CLASS. (of this report) Unclassified	
15a. DECLASSIFICATION/DOWNGRADING SCHEDULE		
16. DISTRIBUTION STATEMENT (of this Report) Distribution of this document is unlimited.		
17. DISTRIBUTION STATEMENT (of the abstract entered in Block 20, if different from Report)		
18. SUPPLEMENTARY NOTES		
19. KEY WORDS (Continue on reverse side if necessary and identify by block number) Grain boundary segregation Magnesium segregation Al-Zn-Mg ternary alloy Auger plasmon-loss		
20. ABSTRACT (Continue on reverse side if necessary and identify by block number) Auger electron spectroscopy (AES) has been used to measure the grain boundary concentration profiles of alloy additions in a Al-5.5% Zn-2.5% Mg ternary. The AES depth profiles show marked segregation of Mg and Zn to the grain boundary, in contrast to that reported previously on similar Al alloys. It is found that this apparent contradiction can be resolved by exploiting the plasmon-loss features of the AES spectra to help elucidate the grain		


GRAIN BOUNDARY SEGREGATION OF A Al-Zn-Mg TERNARY ALLOY

J. M. Chen, T. S. Sun, R. K. Viswanadham and J.A.S. Green

April 1977


ADDITIONAL FOR	
NTIS	White Section <input checked="" type="checkbox"/>
BUC	Buff Section <input type="checkbox"/>
UNANNOUNCED	<input type="checkbox"/>
JUSTIFICATION	
BY	
DISTRIBUTION/AVAILABILITY CODES	
Dist.	Avail. or Special
A	

J. M. Chen, T. S. Sun, R. K. Viswanadham and J. A. S. Green are with
Martin Marietta Laboratories, 1450 South Rolling Road, Baltimore, Mary-
land 21227.



ABSTRACT

Auger electron spectroscopy (AES) has been used to measure the grain boundary concentration profiles of alloy additions in a Al-5.5% Zn-2.5% Mg ternary. The AES depth profiles show marked segregation of Mg and Zn to the grain boundary, in contrast to that reported previously on similar Al alloys. It is found that this apparent contradiction can be resolved by exploiting the plasmon-loss features of the AES spectra to help elucidate the grain boundary segregation. With the AES/plasmon-loss measurements, one can determine not only the concentration of Mg and Zn at the grain boundary, but also the metallurgical environments surrounding the alloy additions. It is shown that, for over-aged specimens of the Al alloy, only a fraction of the total Mg at the grain boundary is incorporated in MgZn_2 precipitates, the remainder being segregated to within a few atomic layers of the boundary.



INTRODUCTION

Grain boundary segregation of alloy components and impurities has been known for some time.¹ The extreme importance of this phenomena to the mechanical properties of metals was not apparent, however, until the advent of Auger electron spectroscopy (AES).²⁻⁴ The shallow probing depth (10-20 Å) of AES revealed that the segregated elements can be localized to the surficial atomic layers of the grain boundary. Thus, AES has been extremely useful in determining the chemical composition of grain boundary surfaces which can then be correlated with other metallurgical properties of materials.

In the case of Al-Zn-Mg alloys, AES studies⁵ have shown that the alloying elements Mg and Zn are heavily segregated to the grain boundaries. Transmission electron microscopy (TEM) studies^{6,7} have shown that for aged Al-Zn-Mg alloys, the segregated elements form MgZn_2 precipitates, and as a consequence, there exists a precipitate free zone (PFZ) at both sides of the grain boundary. The composition and mechanical properties of the PFZ has been the focus of several studies on the stress corrosion of aluminum alloys since cracking in these alloys is intergranular. Recent mechanistic studies⁸⁻¹⁰ have indicated that crack propagation may occur due to hydrogen embrittlement, as opposed to anodic dissolution¹¹ as previously suggested. In conducting additional measurements of the alloy composition immediately adjacent to the grain boundary to further investigate the mechanism of cracking, it became clear that there are considerable contradictions in the literature with regard to grain boundary segregation in these alloys.

For example, Doig and Edington¹²⁻¹⁴ reported measurements of Mg content near the grain boundaries of Al-5.9% Zn-3.2% Mg alloys. By monitoring the plasmon loss of the electron beam in a TEM, Doig and Edington were able to determine the spatial distribution of Mg as the electron beam was traversed across a grain boundary. The situation is depicted by the trace a-a' in Fig. 1(a). For as-quenched specimens, Doig and Edington found an accumulation of Mg at the grain boundary. On the other hand, for over-aged specimens, their measurements showed a depletion of Mg in the PFZ, the Mg content decreasing from the bulk value of 3.2% to about 0.2% at the boundary. Some of Doig and Edington's data¹⁴ is reproduced in Fig. 1(b) and (c). The above results were interpreted with the model that, in the over-aged case, a major portion of Mg at the grain boundary combine to form the $MgZn_2$ precipitates, leaving the region between the precipitates depleted in Mg.

Recently, Green et al.¹⁵ also have measured the chemical composition of similar Ag-Zn-Mg alloys for as-quenched, peak and over-aged conditions. AES and argon ion sputtering were used to obtain the chemical depth profiles of grain boundary surfaces. The AES measurements showed, however, an accumulation of Mg at the grain boundary under all conditions.

In this paper, we demonstrate that the apparent contradiction between the TEM/plasmon loss results of Doig and Edington and the AES results of Green et al. can be resolved by exploiting the plasmon loss features of the AES spectra to help elucidate the segregation/precipitation problem. Specifically, it is found that the plasmon loss energy measurements in the TEM and the AES techniques provide different, but complementary, information about the grain boundary. A combination of these two techniques has led to a better understanding of segregation effects at grain boundaries.

EXPERIMENTAL METHODS AND MATERIALS

The instrument used for the AES study is a Physical Electronics Model 548 Auger/ESCA spectrometer, which features a double-pass cylindrical mirror analyzer and an ultra high vacuum system (UHV). The Auger signal is excited by a 5 KeV primary electron beam from an electron gun housed coaxially inside the analyzer. Most AES measurements were made with a focussed beam of 200 μm diameter and 50 to 60 μA current. The system is equipped with an Ar^+ ion sputtering gun, capable of producing 2 KeV ions. All the experiments were conducted under a basal pressure of less than 5×10^{-10} torr, except during ion sputtering. During sputtering, the UHV system is filled with pure argon to a pressure of 5×10^{-5} torr, while liquid nitrogen is used to cool the lower section of the UHV system via a cryogenic design to further trap oxygen and other impurity gases. The system has a multiplex unit, which enables the peak-to-peak height of six different Auger peaks to be plotted, and is indispensable for monitoring depth profiles. A fracture device, utilizing a shear-to-break configuration was used for the in situ fracture experiments.

To obtain quantitative information from the depth profiles, the peak-to-peak heights of the elements were expressed as a ratio of the peak-to-peak height of the matrix element Al(1396 eV). Conversion from such ratios to approximate atomic percentages requires the use of elemental sensitivities. The peak-to-peak height ratios were then normalized by using the sensitivity factors provided in the "Handbook for Auger Electron Spectroscopy" by Physical Electronics Industries (PHI), Inc.¹⁶

The high purity ternary used for these investigations had a nominal composition of 5.5 wt % Zn and 2.5 % Mg. Strips 1 mm thick were solution treated in dry argon at a temperature of 475°C for 10 mins. and water quenched. The grain size for the solution treatments was about 0.08 mm. The quenched samples were then heat treated at 130°C and 160°C for 0, 4½, and 22 hrs. to obtain the under-, peak-, and over-aged conditions. Small strips were then cut from the samples, notched, and transferred to the spectrometer.

RESULTS

A) Auger Depth Profiles

A scanning electron micrograph of the fractured surface of an aged sample is shown in Fig. 2. The as-quenched samples show a combination of inter- and transgranular fractures. On the other hand, the peak and over-aged samples show definite inter granular fracture. In this paper, we are concerned mainly with the fractured surfaces of aged samples. It is clear from Fig. 2 that AES measurements on these samples will be probing predominantly the grain boundary surfaces.

A typical Auger spectrum taken from the fractured surface of an over-aged sample (160°C for 22 hours) is shown in Fig. 3. The grain boundary depth profiles for Mg and Zn, obtained on the ternary alloy in different heat treated conditions, are shown in Figs. 4 and 5 respectively. The age-hardening curves at these two temperatures are superimposed on the profiles. We note several important features in these figures:

- (i) The Auger spectrum for the over-aged grain boundary surface (Fig. 3) indicates the presence of the alloy additions Mg and Zn. The Auger peak-to-peak amplitudes can be converted to atomic

percentages.¹⁶ Such conversions give ~5.4 atomic % for Mg and ~4.5 atomic % for Zn. If all the Mg and Zn were exclusively due to MgZn_2 precipitates the Mg to Zn ratio should be 1:2. Therefore, it is clear, as already pointed out by Green et al,¹⁵ that in addition to MgZn_2 precipitates, the grain boundary contains excess Mg.

- (ii) The above observation can be substantiated further by comparing Fig. 3 with the Auger spectrum of a MgZn_2 alloy* which is shown in Fig. 6. Such a direct comparison of Auger amplitudes eliminates any uncertainty involved in estimating Auger sensitivities for Mg and Zn. The Zn/Mg Auger peak height ratio in Fig. 3 is about 1:0.75 while that for the MgZn_2 alloy is about 1:0.28. Thus, if we assume that all the Zn atoms on the grain boundary surface of the over-aged sample were incorporated in the second phase particles, then ~40% of the total Mg would be accounted for in the MgZn_2 precipitates themselves and the remaining 60% would be outside the precipitates.
- (iii) As shown in Fig. 4, under all heat treatment conditions, there is a marked segregation of Mg to the grain boundaries. The grain boundary concentrations are several times the bulk concentration. This is in sharp contrast to the results of Doig and Edington as sketched in Fig. 1(b) and (c). They observed a much less dramatic accumulation of Mg at the grain boundary for as-quenched samples and a depletion of Mg for over-aged samples.

*The authors are grateful to Dr. F. Cocks for preparing the sample of MgZn_2 intermetallic.

- (iv) The width of the segregation zone, which can be defined by the point where the Mg concentration decreases to the arithmetic mean between the grain boundary and bulk concentrations, varies from about 10 Å for the as-quenched samples to about 100 Å for the over-aged samples, see Fig. 4. These results are also in contrast to the Doig and Edington data where the width, as measured by the TEM/plasmon loss technique, is about 500 Å.
- (v) Since the plasmon energy of Al alloys depends only weakly on the concentration of Zn addition,¹⁷ the TEM/plasmon loss measurement cannot provide the concentration profile for Zn. As shown in Fig. 5, AES measurements indicate a similar grain boundary segregation of Zn. In the over-aged cases, however, the depth profile for Zn is distinctively different. Instead of a very rapid initial decrease, it shows a plateau at the grain boundary. As a consequence, the segregation is extended to about 200 Å.

B) Plasmon Loss of Auger Electrons

In AES measurements on metallic surfaces, one measures not only the Auger electrons ejected into the vacuum without energy loss, but also the Auger electrons that have suffered plasmon losses. The latter give rise to a satellite peak on the low energy side of the Auger peak. Its energy position relative to the Auger peak is determined by the plasmon energy and can be measured accurately. Since the plasmon energy is a function of the electron density of the medium that the escaping Auger electrons penetrate, the Auger electron-induced plasmon loss satellites can provide

information about the environment surrounding the particular chemical species of interest. In particular, the plasmon energy losses measured in Al and in MgZn_2 alloy are 15.8 ± 0.2 and 12.0 ± 0.2 eV respectively. Thus, an energy loss of 15.8 eV should be observed for the Mg atoms in solution near the grain boundary and an energy loss of 12.0 eV for the Mg atoms in the MgZn_2 precipitates.

Figure 7 shows portions of high resolution Auger spectra of Al-Zn-Mg alloys. Our focus is on the 994 eV (Zn), 1186 eV (Mg) and 1396 eV (Al) Auger peaks. As indicated, there is a plasmon-loss satellite associated with each Auger peak, and the plasmon energy losses are different for as-quenched and over-aged conditions. The Auger spectrum for the sputtered condition was obtained after sufficient material on the grain boundary was removed by Ar ion bombardment until the bulk composition of the alloy was reached.

The plasmon energy losses for the Al-Zn-Mg alloys, together with that for MgZn_2 , are summarized in Table I. We note several interesting points:

- (i) The plasmon loss energy for the Al Auger peak is constant at 15.8 ± 0.2 eV for as-quenched, over-aged and sputtered samples. This is understandable because the alloy additions constitute only a few percent of the Al alloy, so the majority of Al Auger electrons escape through a medium of essentially pure Al metal.
- (ii) For the over-aged samples, the plasmon loss energy for the Mg Auger peak is 13.3 ± 0.2 eV, appreciably higher than that in MgZn_2 (12.0 ± 0.2 eV), and increases to 15.3 ± 0.2 eV when the

bulk of the grain is reached after sputtering. We believe this result is significant. It provides additional support to the picture that only a fraction of the total Mg at the grain boundary is associated with MgZn_2 , the rest is at the grain boundary situated outside of the precipitates.

- (iii) The plasmon losses for the as-quenched samples do not change on sputtering. Thus, although there is an appreciable segregation of both Mg and Zn to the grain boundary for the as-quenched samples, the chemical states of Mg and Zn appear to be the same at the grain boundary as in the bulk.
- (iv) For the over-aged samples, the plasmon loss energy for the Zn Auger peak is 12.4 ± 0.2 eV, nearly the same as that measured in MgZn_2 . This result suggests that, for the over-aged samples, all the Zn atoms at the grain boundary are in the MgZn_2 precipitates.

The plasmon loss in the as-quenched samples (14.4 ± 0.2 eV for Zn and 15.4 ± 0.2 eV for Mg), are consistently lower than that for Al (15.8 ± 0.2 eV). This suggests that even for as-quenched samples there is some degree of precipitate formation (probably Guinier-Preston zones) throughout the bulk of the material.

DISCUSSION

The above AES plasmon loss results indicate that, at the grain boundary of over-aged samples, the Zn atoms are all in the form of MgZn_2 precipitates. On the other hand, only about 40% of total Mg is in the precipitates, the other 60% of Mg being localized to within a few atomic layers of the grain

boundary. In this section, we will utilize these findings in an attempt to resolve the apparent contradiction between the TEM / plasmon-loss and the AES / plasmon loss data.

An important factor that must be taken into consideration when comparing the AES and TEM data is the vast difference in spatial resolution of these two techniques. In TEM, the electron beam is typically less than 100 Å in diameter while the electron beam used in our Auger measurement was about 200 μm in diameter. Therefore, the Auger data represent a measure of Mg content averaged over an area of 200 μm in diameter on the fracture surface, which corresponds to about 10 grains for the grain size employed (~.08 mm). On the other hand, the TEM Mg profile was obtained by traversing the 100 Å electron beam across the grain boundary in between the MgZn₂ precipitates¹² as depicted in Fig. 1(a). Therefore, when interpreting the AES data, the contribution from the MgZn₂ precipitates should certainly be included.

Also, due to experimental limitations, the TEM technique is not capable of measuring Mg content to within 50 Å of the grain boundary. Therefore, any accumulation of Mg localized to within a few atomic layers of the grain boundary will not be detected by the TEM / plasmon loss measurement. On the other hand, the AES technique, being a surface sensitive tool, is ideally suited to detect just such accumulations.

The TEM / plasmon-loss technique measures the Mg concentration within the grains, but not the Mg concentration at the grain boundary, while the AES depth profile includes contributions from both. Therefore, to interpret the AES Mg depth profile data, we should add to the concentration profile of Doig and Edington the contributions from the precipitates as well as the

Mg localized at grain boundary. Since we have deduced from the plasmon-loss satellite measurement that for the over-aged samples, all of Zn at the grain boundary is incorporated in the precipitates, we conclude from the Auger peak-to-peak amplitude information of Figs. 3 and 6 that about 40% of Mg is associated with MgZn_2 and the remainder is outside the precipitates.

A schematic illustration of the various contributions to the Mg depth profile of the over-aged samples is shown in Fig. 8(a). The total Mg profile (curve a) is the sum of the profile at the grain boundary (curve b), the profile within the grain (curve c) and the profile of the precipitate (curve d). As outlined in the following paragraphs, the width of curve d is estimated from the measured concentration profile for Zn. As seen, the total Mg profile resembles closely those shown in Fig. 4.

Similarly, we can construct a Mg depth profile for the as-quenched samples. Because of the absence of grain boundary precipitates in this case, the profile can be obtained by simply adding to the profile within the grain of Doig and Edington (curve c) a narrow profile representing the grain boundary Mg contribution (curve b). This is shown in Fig. 8(b). Note that due to the absence of precipitates, the total Mg profile in Fig. 8(b) is steeper than that of Fig. 8(a), consistent with the AES data on Fig. 4. Thus, by taking into account the various contributions to the Mg depth profile, the apparent contradiction between the TEM/plasmon-loss and AES measurement can be resolved.

As pointed out in Section A, for the over-aged samples, the depth profiles for Zn show a plateau at the grain boundary. In light of the above discussion, this is now easily understandable: in the over-aged cases, all

the Zn atoms are incorporated in the MgZn_2 precipitates. The AES depth profile simply maps out the concentration profile of the precipitates. The as-quenched samples as well as the 130°C , 4.5 hour aged sample do not have grain boundary precipitates (Fig. 5). On the other hand, the samples aged at 130°C for 22 hours, 160°C for 4.5 hours and 22 hours show clear evidence of precipitate formation. The size of the precipitates, as shown in Fig. 5, is about 200 Å. This information was used to estimate the width of the precipitate-contribution to the total Mg profile (Fig. 8(a)).

SUMMARY AND CONCLUSIONS

AES measurements have been used to determine the concentration profiles of Mg and Zn at grain boundaries of an Al-Zn-Mg ternary under different aging conditions. The AES depth profiles show sharp segregation of Mg and Zn to the grain boundary, more marked than reported by Doig and Edington on similar Al alloys. In the case of samples containing precipitates, the AES results were in apparent contradiction to those reported by Doig and Edington using TEM/plasmon-loss measurements.

We have shown that plasmon energy losses in the Auger spectrum can be exploited to help elucidate the precipitation/segregation picture. With the measured Auger amplitude and plasmon-loss information, we are able to determine not only the concentration of Mg and Zn at the grain boundary but also the chemical environments of the alloying additions.

It is found that, for both the as-quenched and over-aged samples, there is a marked segregation of Mg and Zn to the grain boundary; and that for the over-aged samples about 40% of the total Mg at the grain boundary is incorporated in MgZn_2 precipitates while the remaining Mg is segregated to within a few atomic layers of the grain boundary.

Based on the above information, together with the recognition that TEM/plasmon-loss and AES techniques measure different aspects of the grain boundary, it is possible to resolve the apparent contradictions between the results of these two techniques. These two techniques provide different, but complementary information, about the grain boundary. A combination of these techniques has led to an improved picture of grain boundary segregation in Al-Zn-Mg alloys.

ACKNOWLEDGEMENT

The authors acknowledge the financial support of the Office of Naval Research (Contract No. N00014-74-C-0277) and are grateful to P. A. Clarkin for his constant encouragement.

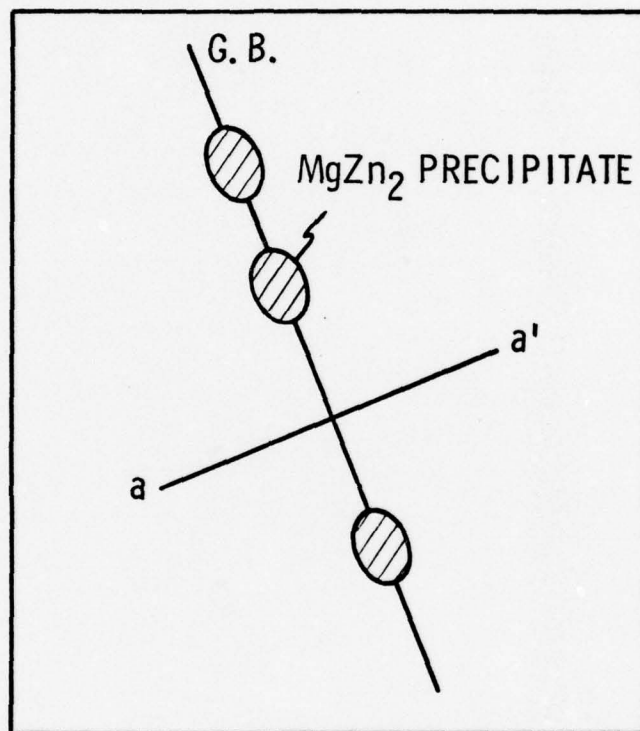
Table I. Measured plasmon loss energies in MgZn_2 and Al-Zn-Mg alloys

	Zn	Mg	Al
MgZn_2	$12.0 \pm 0.2 \text{ eV}$	12.0 ± 0.2	-
Al-Zn-Mg as quenched	14.4 ± 0.2	15.4 ± 0.2	15.8 ± 0.2
Al-Zn-Mg over aged	12.4 ± 0.2	13.3 ± 0.2	15.7 ± 0.2
Al-Zn-Mg sputtered	14.5 ± 0.2	15.3 ± 0.2	15.8 ± 0.2

REFERENCES

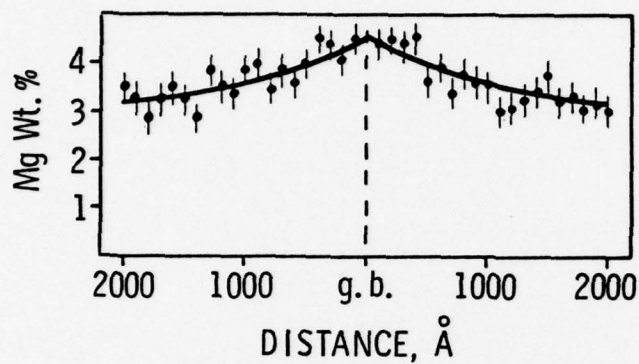
1. J. H. Westbrook: Met. Rev., 1964, vol. 9, p.415.
2. M. L. Marcus and P. W. Palmberg: Trans. AIME, 1969, vol. 245, p. 1664.
3. D. F. Stein, A. Joshi and R. P. LaForce: Trans. ASM, 1969, vol. 62, p. 776.
4. H. Ohtani, H. C. Feng and C. J. McMahon, Jr.: Met. Trans., 1974, vol. 5, p. 516.
5. J. A. S. Green and W. G. Montague: Corrosion, 1975, vol. 31, p. 209.
6. A. Kelly and R. B. Nicholson: Progress Mat. Sci., 1963, vol. 10, p. 151.
7. A. J. Cornish and M. K. B. Day: J. Institute of Metals, 1969, vol. 97, p. 44.
8. J. A. S. Green, H. W. Hayden and W. G. Montague, "Effect of Hydrogen on Behavior of Materials," Ed. A. W. Thompson and I. M. Bernskin, Publ. Met. Soc. AIME, 1976, p. 200.
9. G. M. Scamans, R. Alain and P. R. Swann, Corrosion Sci., 16 (7), 443 (1976).
10. R. J. Gest and A. R. Troiano, Corrosion, 30, 274 (1974)
11. A. J. Sedricks, J. A. S. Green and D. L. Novak "Stress Corrosion Cracking of Al-Zn-Mg Alloys." In: "The Corrosion Behavior of Grain Boundary Constituents." Paper presented at 5th Intl. Cong. on Metallic Corrosion, Tokyo, May 1972.

12. P. Doig and J. W. Edington: Brit. Corrosion J. (Quarterly), 1974, vol. 9, p. 220.
13. P. Doig and J. W. Edington: Brit. Corrosion J. (Quarterly), 1974, vol. 9, p. 461.
14. P. Doig and J. W. Edington: Met. Trans. 6A, 1975, p. 943.
15. J.A.S. Green, R. K. Viswanadham, T. S. Sun and W. G. Montague: Corrosion, submitted for publication.
16. P. W. Palmberg, G. E. Riach, R. E. Weber and N. C. MacDonald: "Handbook of Auger Electron Spectroscopy," p. 14, Physical Electronics Industries., Edina, Minnesota, 1976.
17. R. F. Cook and S. L. Cundy: Phil. Mag., 1969, vol. 20, p. 665.

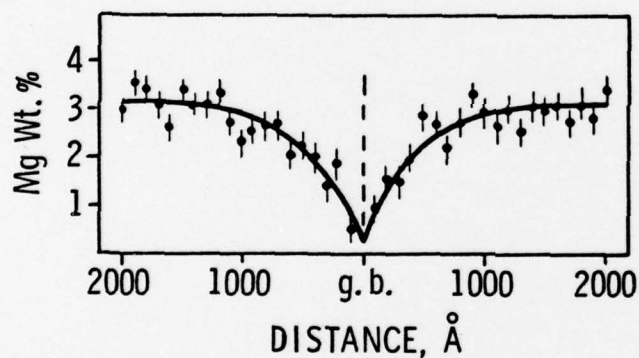


(a)

Fig. 1(a) Schematic diagram of MgZn_2 precipitates at a grain boundary, $a-a'$ represents the line along which microanalysis of Mg concentration is performed by the TEM/plasmon loss technique.



(b)
WATER QUENCHED
FROM 500°C



(c)
AIR COOLED
FROM 500°C

ANALYSIS ACROSS BOUNDARY OF
Al - 5.9 Zn - 3.2 Mg ALLOY (DOIG AND EDINGTON)

Fig. 1(b) and 1(c). Mg concentration profiles across grain boundaries
in Al-5.9% Zn-3.2% Mg alloys as measured by Doig and Edington (ref. 14).



Fig. 2. Scanning electron micrograph of the fracture surface of a quenched and aged high purity Al-Zn-Mg ternary alloy. The grain size is approximately 0.08 mm ($\times 100$).

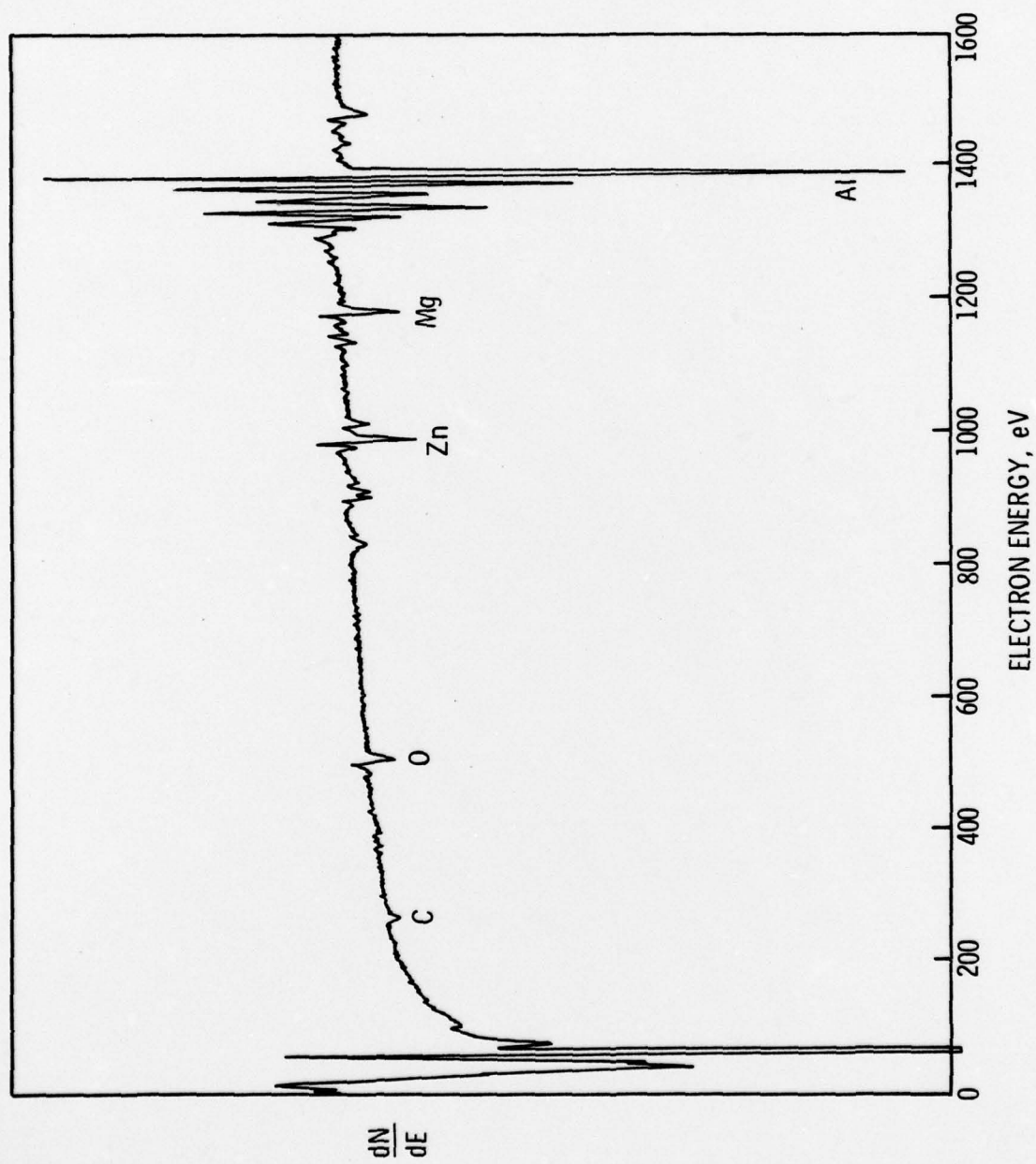


Fig. 3. Auger electron spectrum from the fracture surface of an over-aged high purity ternary alloy.

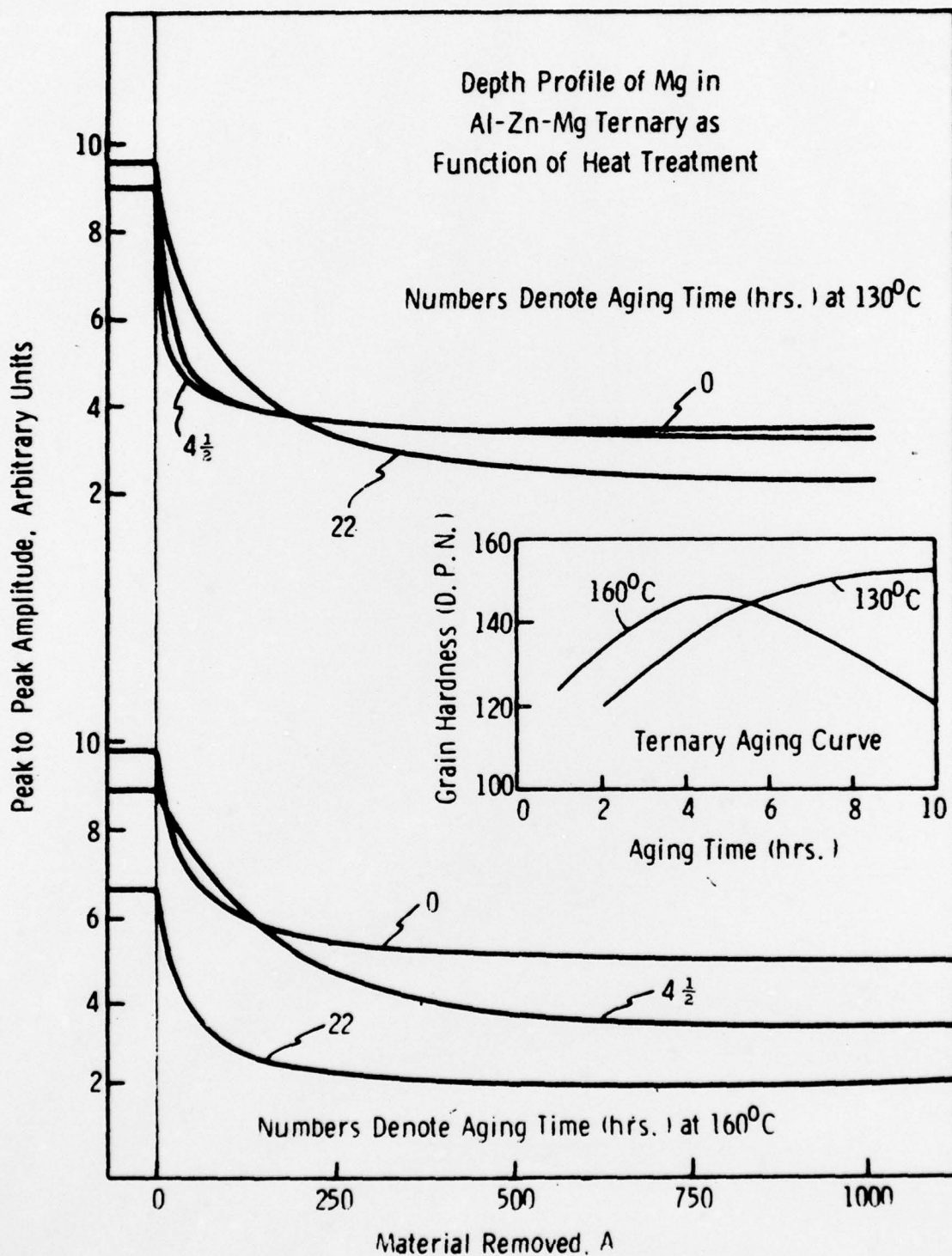


Fig. 4. Chemical depth profiles for Mg in Al-Zn-Mg ternary alloys as a function of heat treatment. The aging curves at 130°C and 160°C are superimposed.

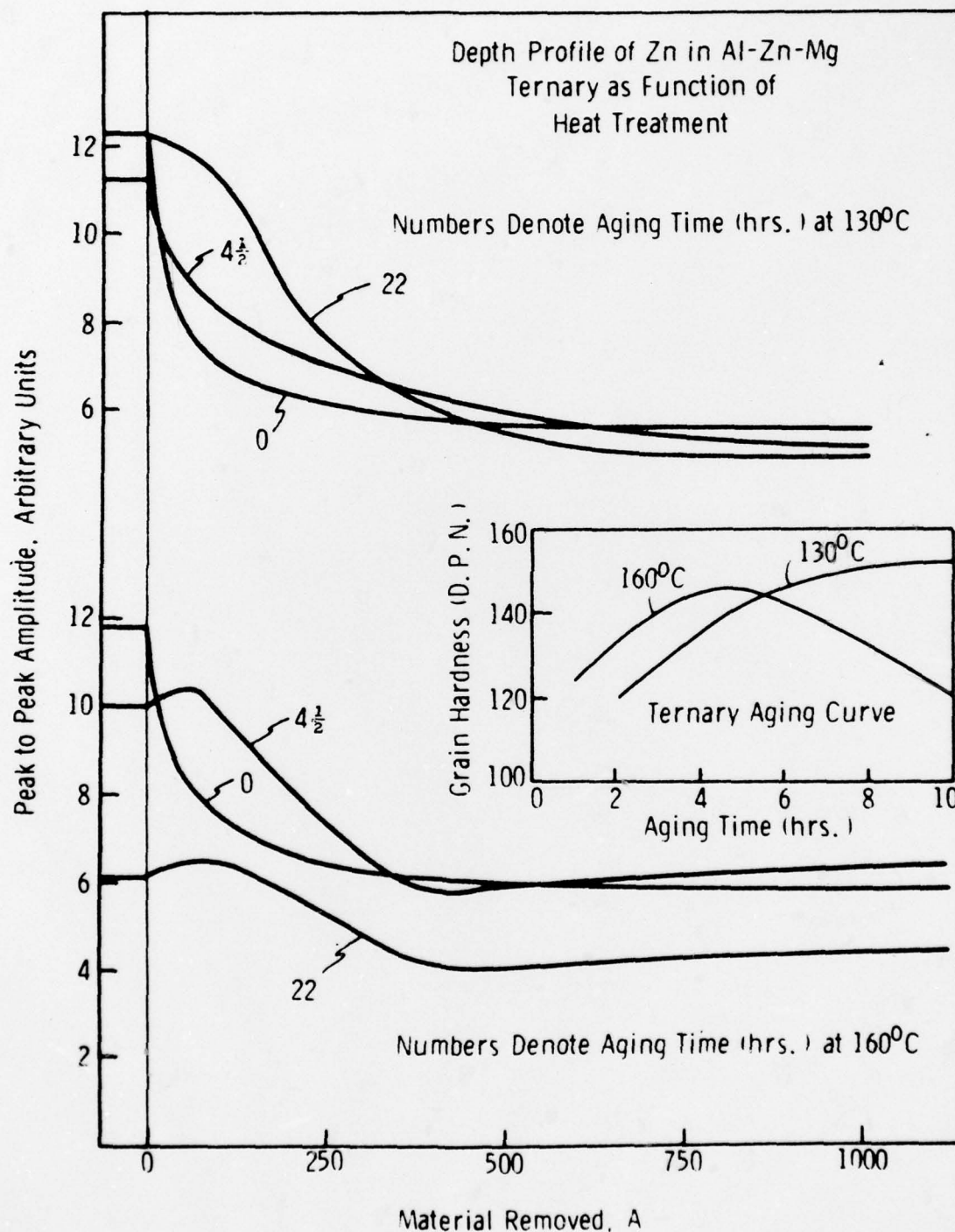


Fig. 5. Chemical depth profiles for Zn in Al-Zn-Mg alloys as a function of heat treatment. The aging curves are superimposed.

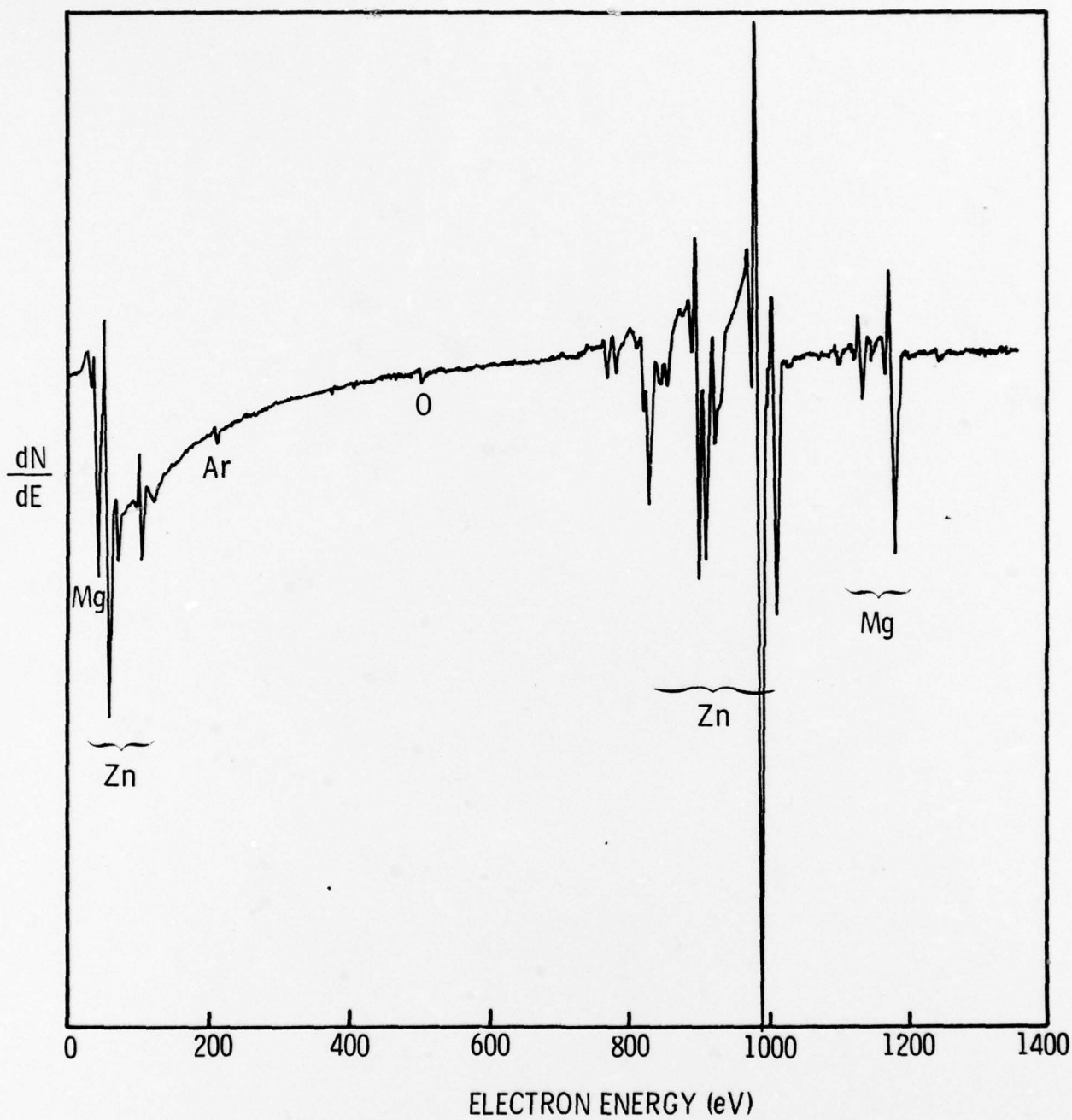


Fig. 6. Auger electron spectrum of a MgZn_2 alloy surface.

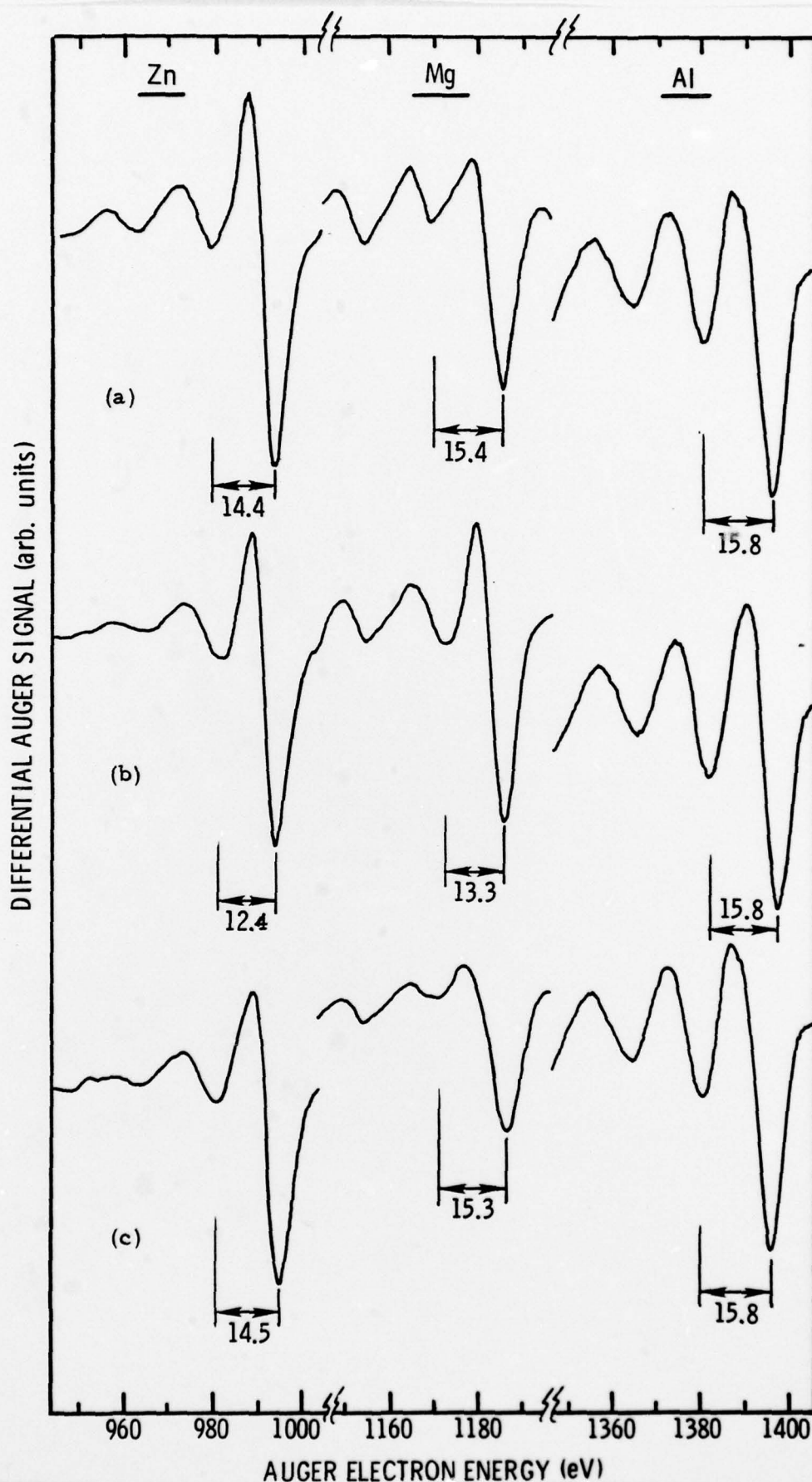


Fig. 7. Auger electron spectra for the elements Zn, Mg and Al of the Al-Zn-Mg alloy in as-quenched (row (a)) and over-aged (row (b)) conditions. The spectra representing the bulk of the alloy is shown in row (c).

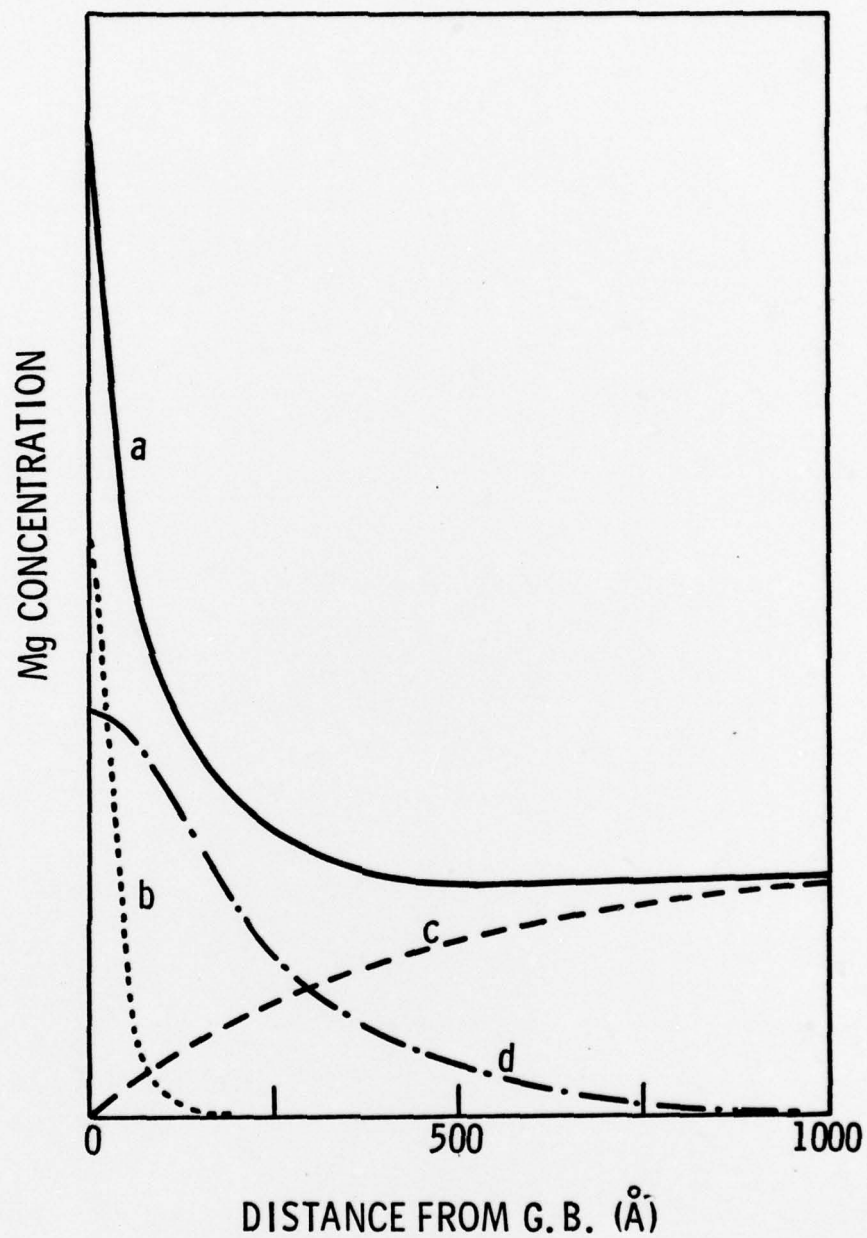


Fig. 8(a). Schematic diagram of various contributions to the Mg depth profile for over-aged samples.

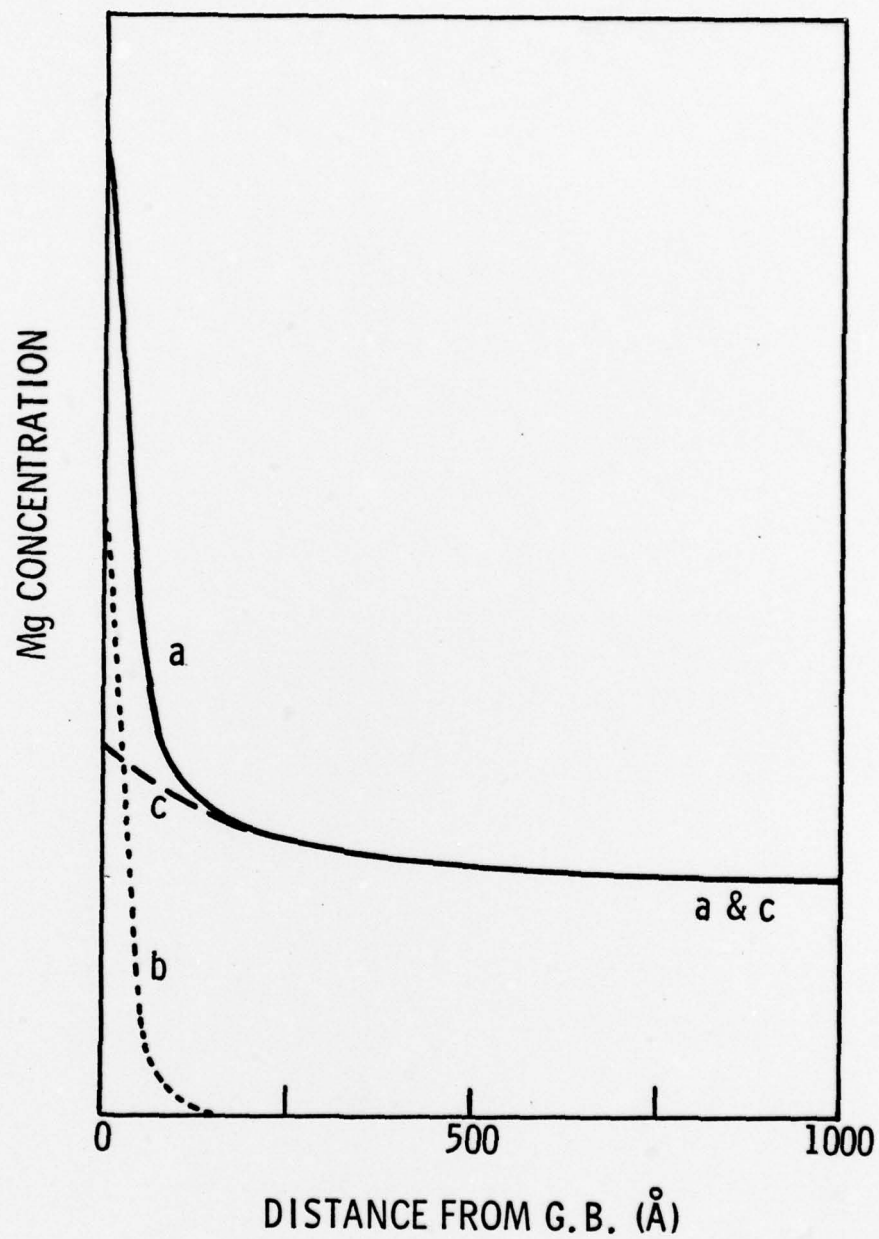


Fig. 8(b). Schematic diagram of various contributions to the Mg depth profile for as-quenched samples.

BASIC DISTRIBUTION LIST

August 1974

Technical and Summary Reports			
<u>Organization</u>	<u>No. of Copies</u>	<u>Organization</u>	<u>No. of Copies</u>
Defense Documentation Center Cameron Station Alexandria, Virginia 22314	(12)	Naval Air Propulsion Test Center Trenton, New Jersey 08628 Attn: Library	(1)
Office of Naval Research Department of the Navy Arlington, Virginia 22217 Attn: Code 471 Code 105 Code 470	(3) (6) (1)	Naval Weapons Laboratory Dahlgren, Virginia 22448 Attn: Research Division	(1)
Director Office of Naval Research Branch Office 495 Summer Street Boston, Massachusetts 02210	(1)	Naval Construction Battalion Civil Engineering Laboratory Port Hueneme, California 93043 Attn: Materials Division	(1)
Director Office of Naval Research Branch Office 536 South Clark Street Chicago, Illinois 60605	(1)	Naval Electronics Laboratory Center San Diego, California 92152 Attn: Electronic Materials Sciences Division	(1)
Office of Naval Research San Francisco Area Office 760 Market Street Room 447 San Francisco, California 94102	(1)	Naval Missile Center Materials Consultant Code 3312-1 Point Mugu, California 93041	(1)
Naval Research Laboratory Washington, D. C. 20390		Commanding Officer Naval Ordnance Laboratory White Oak Silver Spring, Maryland 20910 Attn: Library	(1)
Attn: Code 6000 Code 6100 Code 6300 Code 6400 Code 2627	(1) (1) (1) (1) (6)	Naval Ship R&D Center Materials Department Annapolis, Maryland 21402	(1)
Attn: Mr. F. S. Williams Naval Air Development Center Code 302 Warminster, Pennsylvania 18974	(1)	Naval Undersea Center San Diego, California 92132 Attn: Library	(1)
		Naval Underwater System Center Newport, Rhode Island 02840 Attn: Library	(1)

BASIC DISTRIBUTION LIST (Cont'd)

August 1974

<u>Organization</u>	<u>No. Of Copies</u>	<u>Organization</u>	<u>No. of Copies</u>
Naval Weapons Center China Lake, California 93555 Attn: Library	(1)	Commanding General Department of the Army Frankford Arsenal Philadelphia, Pennsylvania 19137 Attn: ORDBA-1320	(1)
Naval Postgraduate School Monterey, California 93940 Attn: Materials Sciences Dept.	(1)	Office of Scientific Research Department of the Air Force Washington, D. C. 20333 Attn: Solid State Div. (SRPS)	(1)
Naval Air Systems Command Washington, D. C. 20360 Attn: Code 52031 Code 52032 Code 320	(1) (1) (1)	Aerospace Research Labs Wright-Patterson AFB Building 450 Dayton, Ohio 45433	(1)
Naval Sea System Command Washington, D. C. 20362 Attn: Code 035	(1)	Air Force Materials Lab (LA) Wright-Patterson AFB Dayton, Ohio 45433	(1)
Naval Facilities Engineering Command Alexandria, Virginia 22331 Attn: Code 03	(1)	NASA Headquarters Washington, D. C. 20546 Attn: Code RRM	(1)
Scientific Advisor Commandant of the Marine Corps Washington, D. C. 20380 Attn: Code AX	(1)	NASA Lewis Research Center 21000 Brookpark Road Cleveland, Ohio 44135 Attn: Library	(1)
Naval Ship Engineering Center Department of the Navy Washington, D. C. 20360 Attn: Director, Materials Sciences	(1)	National Bureau of Standards Washington, D. C. 20234 Attn: Metallurgy Division Inorganic Materials Div.	(1) (1)
Army Research Office Box CM, Duke Station Durham, North Carolina 27706 Attn: Metallurgy & Ceramics Div.	(1)	Atomic Energy Commission Washington, D. C. 20545 Attn: Metals & Materials Branch	(1)
Army Materials and Mechanics Research Center Watertown, Massachusetts 02172 Attn: Res. Programs Office (AMXMR-P)	(1)	Defense Metals & Ceramics Information Center Battelle Memorial Institute 505 King Avenue Columbus, Ohio 43201	(1)

BASIC DISTRIBUTION LIST (Cont'd)

August 1974

<u>Organization</u>	<u>No. of Copies</u>	<u>Organization</u>	<u>No. of Copies</u>
Director Ordnance Research Laboratory P. O. Box 30 State College, Pennsylvania 16801	(1)		
Director Applied Physics Lab. University of Washington 1013 Northeast Fortieth Street Seattle, Washington 98105	(1)		
Metals and Ceramics Division Oak Ridge National Laboratory P. O. Box X Oak Ridge, Tennessee 37830	(1)		
Los Alamos Scientific Lab. P. O. Box 1663 Los Alamos, New Mexico 87544 Attn: Report Librarian	(1)		
Argonne National Laboratory Metallurgy Division P. O. Box 229 Lemont, Illinois 60439	(1)		
Brookhaven National Laboratory Technical Information Division Upton, Long Island New York 11973 Attn: Research Library	(1)		
Library Building 50 Room 134 Lawrence Radiation Laboratory Berkeley, California	(1)		

C
April 1976

SUPPLEMENTARY DISTRIBUTION LIST

Technical and Summary Reports

Dr. T. R. Beck
Electrochemical Technology Corporation
10035 31st Avenue, NE
Seattle, WA 98125

Dr. David K. Benson
Midwest Research Institute
425 Volker Boulevard
Kansas City, MO 64110

Professor I. M. Bernstein
Carnegie-Mellon University
Schenley Park
Pittsburgh, PA 15213

Professor H. K. Birnbaum
University of Illinois
Department of Metallurgy
Urbana, IL 61801

Dr. B. F. Brown
The American University
Department of Chemistry
Washington, DC 20016

Dr. Otto Buck
Rockwell International
1049 Camino Dos Rios
P.O. Box 1085
Thousand Oaks, CA 91360

Dr. David L. Davidson
Southwest Research Institute
8500 Culebra Road
P.O. Drawer 28510
San Antonio, TX 78284

Dr. J. A. Davis
Bell Aerospace Company
Division of Textron
Buffalo, NY 14240

Dr. D. J. Duquette
Department of Metallurgical Engineering
Rensselaer Polytechnic Institute
Troy, NY 12181

Professor R. T. Foley
The American University
Department of Chemistry
Washington, DC 20016

Professor J. P. Hirth
Ohio State University
Metallurgical Engineering
Columbus, OH 43210

Dr. D. W. Hoepfner
University of Missouri
College of Engineering
Columbia, MO 65201

Dr. G. K. Hubler
Naval Research Laboratory
Washington, DC 20375

Dr. F. Mansfeld
Rockwell International
Science Center
1049 Camino Dos Rios
P.O. Box 1085
Thousand Oaks, CA 91360

Professor H. W. Pickering
Pennsylvania State University
Department of Material Sciences
University Park, PA 16802

Professor Carolyn M. Preece
Bell Laboratories
600 Mountain Avenue
Murray Hill, New Jersey 07974

SUPPLEMENTARY DISTRIBUTION LIST
(Cont'd)

Professor R. W. Staehle
Ohio State University
Department of Metallurgical Engineering
Columbus, OH 43210

Professor E. D. Verink, Jr.
University of Florida
Department of Metallurgical and
Materials Engineering
Gainesville, FL 32601

Dr. R. P. Wei
Lehigh University
Institute for Fracture and
Solid Mechanics
Bethlehem, PA 18015

Professor H. G. F. Wilsdorf
University of Virginia
Department of Materials Science
Charlottesville, VA 22903

Assistant Chief for Technology
Office of Naval Research, Code 200
Arlington, Virginia 22217

Linda Husted
Librarian
Materials Sciences Corporation
Merion Towle Building
Blue Bell, Pennsylvania 19422

Mr. Gregory B. Barthold
Manager, Technical Programs
Aluminum Company of America
1200 Ring Building
Washington, D. C. 20036